Eur. Phys. J. E **10**, 175–189 (2003)
DOI: 10.1140/epje/e2003-00022-1

THE EUROPEAN PHYSICAL JOURNAL E

Vesicles in haptotaxis with hydrodynamical dissipation

I. Cantat[1,2,a], K. Kassner[3], and C. Misbah[1]

[1] Laboratoire de Spectrométrie Physique, Université Joseph Fourier (CNRS), Grenoble I, BP 87, Saint-Martin d'Hères, 38402 Cedex, France
[2] GMCM, Université de Rennes (CNRS), Campus de Beaulieu, bâtiment 11A CS 74205, 263 avenue du Général Leclerc, 35042 Rennes Cedex, France
[3] Institut für Theoretische Physik, Otto-von-Guericke-Universität Magdeburg, Postfach 4120, 39016 Magdeburg, Germany

Received 24 June 2002 and Received in final form 4 February 2003
Published online: 16 April 2003 –

Abstract. We analyze the problem of vesicle migration in haptotaxis (a motion directed by an adhesion gradient), though most of the reasoning applies to chemotaxis as well as to a variety of driving forces. A brief account has been published on this topic [6]. We present an extensive analysis of this problem and provide a basic discussion of most of the relevant processes of migration. The problem allows for an arbitrary shape evolution which is compatible with the full hydrodynamical flow in the Stokes limit. The problem is solved within the boundary integral formulation based on the Oseen tensor. For the sake of simplicity we confine ourselves to 2D flows in the numerical analysis. There are basically two regimes (i) the tense regime where the vesicle behaves as a "droplet" with an effective contact angle. In that case the migration velocity is given by the Stokes law. (ii) The flask regime where the vesicle has a significant (on the scale of the vesicle size) contact curvature. In that case we obtain a new migration law which substantially differs from the Stokes law. We develop general arguments in order to extract analytical laws of migration. These are in good agreement with the full numerical analysis. Finally we mention several important future issues and open questions.

PACS. 87.17.Jj Cell locomotion; chemotaxis and related directed motion – 87.16.Dg Membranes, bilayers, and vesicles – 47.55.Dz Drops and bubbles

1 Introduction

Vesicles are closed membranes suspended in an aqueous solution (Fig. 1). These membranes serve as an efficient permeability barrier. Vesicles mimic one of the most primitive and mechanically flexible dividing interface between the interior and the exterior of a cell. In general, the enclosed fluid is incompressible so that the vesicle evolves at a constant volume. In addition, the membrane exchanges no phospholipid molecules with the solution, so that its area remains constant as time elapses. In its equilibrium state the vesicle is described by a bending energy due to Helfrich [1], which is compatible with the above constraints (constant volume and constant area). Despite its relative simplicity, this model produces a variety of equilibrium shapes, such as stomatocytes, discocytes (bearing resemblance with red blood cells), as well as shapes with higher topology (such as n-genus torus) that have also been observed experimentally [2].

One of the new emerging field of research concerns the elucidation of non-equilibrium features of vesicles. These questions have recently known an increasing interest. Works have been directed towards out-equilibrium fluctuations [3], vesicle alignments in a shear flow [4], vesicle migration close to a substrate [5,6] or in a gravity field [7], lift force [8–10], and vesicle tumbling [11]. Several experiments have dealt recently with vesicle migration [12–15].

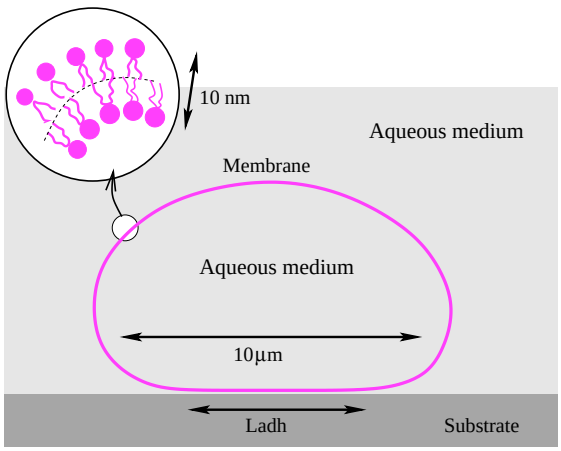

Fig. 1. A schematic view of a vesicle showing the microscopic structure: a bilayer of phospholipidic molecules. The membrane is adhered on the area $\pi\,(L_{\rm adh}/2)^2$.

[a] e-mail: isabelle.cantat@univ-rennes1.fr

Vesicle migration involves hydrodynamical dissipation in the surrounding fluid as well as inside the vesicle, and, in principle, between the two monolayers which may slide with respect to each other. In addition, during motion on a substrate the vesicle dynamics may be limited not only by hydrodynamical flow but also by a breaking and restoring of bonds on the substrate. The slowest mechanism will limit the motion. In this paper we concentrate on the situation where hydrodynamics are the limiting factors and we shall assign no dissipation associated with bonds on the substrate. Of course this is a question of great importance and it will constitute the topic of a future work.

In this paper we shall present an extensive discussion on the problem of haptotaxis (a motion induced by an adhesion gradient), but it will become clear that the modeling will work perfectly well with any other driving force. We determine the main ingredients (adhesion area, etc.) that play a role in the process by which motion takes place. We derive scaling laws on the basis of general dimensional considerations, and compare our results with the full numerical calculation based on the boundary integral formulation. The scheme of the paper is as follows. In Section 2 we introduce the main vesicle properties which are relevant in the present model. In Section 3 we shall first analyze the adhesion properties at equilibrium. Section 4 is devoted to the dynamical model equations and to the integral boundary formulation based on the Green's function techniques. In Section 5 we briefly sketch the numerical scheme. Section 6 deals with the full migration law both analytically and numerically. The results and perspectives are presented in Section 7.

2 Vesicle properties

We consider a vesicle which is initially adhering on a flat surface. An adhesion gradient is prescribed along the substrate. The vesicle moves in the direction of increasing adhesion energy (see Fig. 2). Before dealing with the full dynamical problem, we first discuss the main equilibrium features which are relevant for the model.

2.1 Curvature energy

As stated before, our numerical simulations have been performed in 2D, for the sake of simplicity and of computing time. In a recent work [10], it has been shown that vesicles under shear flow close to a substrate behave in very much the same way as that found in two dimensional simulations, on which we have reported briefly in reference [8]. Thus we believe that the 2D assumption captures the essential features of the 3D vesicle. The 2D assumption means that the vesicle is assumed to be invariant in the z direction, and its shape is simply represented by a closed curve $\mathcal{C}$ in the (x, y) plane. The well known Helfrich curvature energy [1] has then the dimension of an energy per unit length and is written as

$$E_{\rm c} = \frac{\kappa}{2} \int_{\mathcal{C}} c^2 \, {\rm d}s \,, \tag{1}$$

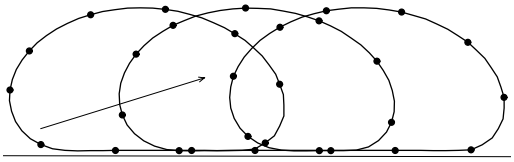

Fig. 2. Stationary vesicle profiles, moving from the left (smaller adhesion) to the right (stronger adhesion); a few discretisation points are represented and the arrow allows to follow one of these at three successive times. This illustrates the rolling and sliding components of the motion.

with κ the membrane rigidity and c the vesicle curvature (counted as positive for a convex shape; *e.g.* for a circle).

The curvature force experienced by a piece of the membrane having an extent ds is obtained upon a functional differentiation. We obtain, with $\mathbf{n}$ being the outward normal vector, the following expression [16]:

$$\mathbf{f}_{\rm c} = -\delta E_{\rm c}/\delta \mathbf{r}(s) = \kappa \left(\frac{\partial^2 c}{\partial s^2} + \frac{c^3}{2} \right) \mathbf{n} \,. \tag{2}$$

That the force has only a normal component is not a surprise. Indeed this is due to the fact that the curvature energy only depends on geometrical properties, which remain unchanged under a purely tangential displacement [17].

2.2 Adhesion energy

The membrane/substrate interaction is characterized by a short range adhesion potential (see Fig. 3). Any form of the potential can be accounted for here. For definiteness we choose the following expression:

$$w(\mathbf{r}) = \bar{w}(x) \left(\frac{d_0}{y} \right)^2 \left[\left(\frac{d_0}{y} \right)^2 - 2 \right], \tag{3}$$

where d_0 is the interaction range of the order of 50 nm [18]. $\bar{w}$ is the local adhesion energy, which depends on x for an inhomogeneous substrate. Typically, we shall set $\bar{w} = w_0 + (x - x_{\rm m})\delta w$. The quantity w_0 is the typical adhesion energy, $x_{\rm m}$ is the center of the adhesion contact, δw represents the difference in the adhesion potential on both sides of the vesicles (the adhesion gradient). The magnitude of the interaction potential depends on the physical nature of the interaction. We will focus on the so-called *weak adhesion* range, between 10^2 and 10^4 kT/μm^2. For example, an adhesion potential of the order of 4 000 kT/μm^2 is observed for physical interactions between neutral membranes [18–21]. Of considerable interest is also the specific interactions due to protein/protein bounds, which prevail in biological situations. In that case, binding/unbinding transitions give rise to specific dissipation, which is not taken into account in the present work. Indeed our wish is to keep the model in its minimal version in order to identify the role of each process. The study of specific adhesion is the topic of a future work.

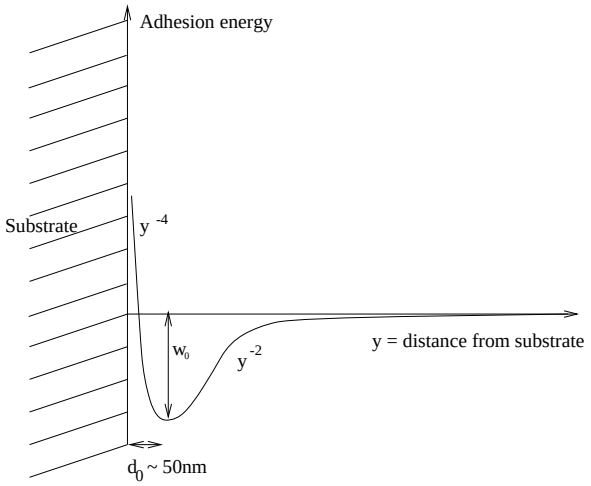

Fig. 3. Vesicle/substrate interaction profile.

Note that we are at liberty to choose an adhesion potential per unit length (in a 2D language) or per unit mass. However, the expression of the force will assume a different form depending on the definition. As this question is somewhat subtle, it deserves a special attention as presented in the following section.

2.3 Local length conservation of the membrane

As stated before, the membrane is composed of insoluble phopholipids in their fluid phase. The bilayer is a 2D *incompressible* fluid. As is the case with bulk fluids, this constraint implies a vanishing velocity divergence. Expressed on a curved surface, this condition not only involves the velocity derivatives, but also the membrane curvature, since the condition is imposed on a curved space. In 2D, the demand of membrane incompressibility implies a local arc-length conservation. The constraint equation couples the normal and tangential membrane velocities, v_n and v_t, to the curvature c, through the following relation (see [17,22]):

$$\mathbf{t}.\frac{\partial \mathbf{v}}{\partial s} = v_\mathrm{n} c + \frac{\partial v_\mathrm{t}}{\partial s} = 0\,. \tag{4}$$

The left hand side clearly shows that this is a divergence along the curve ($\mathbf{t}$ is the tangent unit vector). The right hand side can be obtained by decomposing $\mathbf{v}$ along the normal and the tangent and by using the fact that $\partial\mathbf{n}/\partial s = c\mathbf{t}$ and $\partial\mathbf{t}/\partial s = -c\mathbf{n}$. In order to fulfill at each point of the membrane the incompressibility condition, we introduce a *local* Lagrange multiplier $\zeta(s)$. As this condition ensures the local length conservation (which is a physical constraint), we must supplement the energy of the membrane by a contribution of the form

$$E_\mathrm{l} = \int_\mathcal{C} \zeta(s)\mathrm{d}s\,, \tag{5}$$

from which we get the forces which ensure local incompressibility, upon a functional differentiation:

$$\mathbf{f}_\mathrm{l} = \frac{\partial \zeta}{\partial s}\mathbf{t} - c\zeta\mathbf{n}\,. \tag{6}$$

The function ζ plays the role of an "effective" surface tension. However, care must be taken when making this analogy. In contrast to surface tension at a fluid/fluid interface, the membrane tension is not an intrinsic property of the membrane. It adapts itself to the other forces in order to ensure the local arc-length conservation. As external forces (the adhesion and hydrodynamical forces) depend on time and on space, the effective tension is space and time dependent as well. A local force field tending to extend the membrane leads to a positive tension, whereas if it tends to compress the bilayer, the tension will be negative. Moreover, the tension depends on the precise definition chosen for the other forces. In order to illustrate this subtle question, we find it worthwhile to discuss this point more precisely.

As mentioned above, we are at liberty to choose a potential per unit mass $w_\mathrm{m}(\mathbf{r})$ or per unit surface $w_\mathrm{s}(\mathbf{r})$. The adhesion forces $\mathbf{f}_\mathrm{am}$ and $\mathbf{f}_\mathrm{as}$ associated to both potentials are [16]:

$$\mathbf{f}_\mathrm{am} = -\rho\nabla w_\mathrm{m}(\mathbf{r}) = -\nabla w_\mathrm{s}(\mathbf{r})\,, \tag{7}$$

$$\mathbf{f}_\mathrm{as} = -\left(c\, w_\mathrm{s}(\mathbf{r}) + \frac{\partial w_\mathrm{s}(\mathbf{r})}{\partial \mathbf{n}}\right) n\,, \tag{8}$$

with ρ being the membrane density assumed to be homogeneous and $\rho w_\mathrm{m} = w_\mathrm{s}$. The first functional derivative is performed with respect to a mass variation. We recover here the expected result of a force being proportional to the opposite of the potential gradient. In the second case, a tangential displacement produces no energy change and the tangential forces vanish. On the other hand, once the incompressibility condition is expressed, both models should be completely equivalent. The self-consistency is ensured by the Lagrange multiplier, which takes different values ζ_m and ζ_s in each situation, but they are related to each other by the equation:

$$\zeta_\mathrm{m} = \zeta_\mathrm{s} + w_\mathrm{s}\,. \tag{9}$$

The force experienced by a piece of the membrane is thus an invariant –in that it does not depend on the definition–, as it should be. This can easily be checked from equations (6, 7) and (8). Anyway, the problem of the definition and of the unicity of the "tension" remains.

In principle we can first define the adhesion force before evoking the local length conservation. The adhesion potential is obviously proportional to the number of molecules in interaction: in this spirit this is a potential per unit mass. This potential would be different from the one per unit surface. Both potentials are equivalent only under the condition of local incompressibility. The potential per unit mass seems to be a natural one, since it leads to the conventional definition, $\mathbf{f} = -\nabla w$. We adopt the second convention (per unit surface). This avoids any

mass consideration and leads to a uniform tension under equilibrium. From now on, ζ denotes the Lagrange multiplier corresponding to the model where the potential is defined per unit surface. The correspondence between the two models is straightforward using equation (9).

Summing up (2), (6) and (8) we obtain the total force, with $\mathbf{n}$ and $\mathbf{t}$ the outward normal and tangential vectors, respectively:

$$\mathbf{f}_{\rm memb} = \kappa \left(\frac{\partial^2 c}{\partial s^2} + \frac{c^3}{2} \right) \mathbf{n} + \frac{\partial \zeta}{\partial s} \mathbf{t} - c\zeta \mathbf{n} - \left(c\, w(\mathbf{r}) + \frac{\partial w(\mathbf{r})}{\partial \mathbf{n}} \right) \mathbf{n} \,. \quad (10)$$

2.4 Conservation of the enclosed area

The second conserved quantity is the volume (area in 2D) enclosed by the vesicle. The admitted value for the membrane water permeability is $P_{\rm w} = 10^{-4}$ cm/s [23,24], which is small but not completely negligible. The permeabilities for the solute molecules (sugar, ions, polymer) are much smaller. So, the membrane behaves as a semi-permeable boundary; it allows for osmosis. An area (volume in 3D) variation of, say, $\Delta A/A \sim 1\%$, produces an osmotic pressure $P_{\rm osm} \sim R_{\rm G} T c |\Delta A/A| \sim 1\,000$ Pa for a physiologic osmolarity $c \sim 50$ mMol/L, with $R_{\rm G}$ the universal gas constant and T the temperature. On the other hand, a typical pressure difference produced by curvature forces is $P_{\rm meca} \sim \kappa/R^3 \sim 10^{-1}$ Pa, with $R \sim 1$ μm the typical size of the vesicle. This is too small in order to counterbalance the above osmotic force. Thus there is no resistance to in or out-flow from bending forces.

The impermeability and the area conservation induced by osmotic forces are nevertheless two notions which are distinct, to some extent. Impermeability is a local constraint, whereas the volume conservation is global. A highly permeable vesicle can be pulled in a fluid without any resistance (and without an inner area change), whereas an impermeable one would feel a drag force. The solvent flux through the membrane, $\mathrm{d}A/\mathrm{d}t$, as a function of the pressure difference Δp (in an Onsager-like picture), is given by

$$\frac{\mathrm{d}A}{\mathrm{d}t} \sim P_{\rm w}\, L\, \Delta p \times \frac{V_{\rm mol}}{R_{\rm G} T} \,, \quad (11)$$

with L the vesicle perimeter and $V_{\rm mol}$ the water molar volume. The time scale for permeability depends thus on the driving force. The order of magnitude can vary quite significantly depending on whether an osmotic shock is present or not. For example, the time needed for significantly emptying a vesicle in the presence of an osmotic chock is obtained from equation (11) (with $\Delta p \sim 1\,000$ Pa) to be of order $\tau_{\rm osm} \sim 10^3$ s. This time scale is usually observed for osmotic swelling or de-swelling. On the other hand, the response to a typical pressure difference produced by curvature forces $\kappa/R^3 \sim 10^{-1}$ Pa is $\tau_{\rm perm} \sim 10^7$ s. The latter process can be referred to as the natural permeability. This estimate shows that once the osmolarity is fixed and the swelling factor reached, the vesicle will then evolve without water flux through the membrane on time scales of motions of interest. The assumption of local impermeability is legitimate. This entails that the fluid velocity at the membrane is equal that of the membrane itself.

3 Adhesion length and tension

The adhesion length (or adhesion area in 3D) and the tension are related to the vesicle parameters (swelling, size) in a non trivial way in general, even at equilibrium. A liquid droplet is characterized by its contact angle *via* the Young relation. On a membrane, such an angle discontinuity would produce a huge curvature energy. Thus, an elastic membrane should meet the substrate tangentially. The analogue of the Young condition concerns here the contact curvature, though in some limits this condition has a similar form (see below). For a vesicle at equilibrium on a homogeneous substrate with an adhesion energy $\bar{w}(x) = w_0$ the contact curvature is given by $R_{\rm c} = 1/c_0 = \sqrt{\kappa/2w_0}$ [25,26]. This length scale must be compared with the geometrical length scales (*e.g.* the size of the vesicle). There are two extreme regimes: (i) the tense regime in which the adhesion is strong enough so that the contact radius of curvature $R_{\rm c}$ is small in comparison to the vesicle size, and (ii) the flask regime where $R_{\rm c}$ is large. More precisely, the first regime corresponds to $R \gg R_{\rm c}$ and the second to $R \sim R_{\rm c}$. In the first case, it is possible to define an effective contact angle, in a manner which is similar to the contact angle for a droplet [17,27].

3.1 Adhesion length

This section deals with the derivation of the relation between the adhesion length and other parameters. This length constitutes an essential quantity for the study of dynamics. The adhesion length, $L_{\rm adh}$, is defined in Figure 1. This quantity is well defined as long as the range of the adhesion potential is small in comparison to the vesicle size, $d_0 \ll R$. There are two interesting regimes that will be discussed separately.

3.1.1 The tense regime: $R_{\rm c} \ll R$

This regime is achieved for strong adhesion, or a small rigidity, or giant vesicles. In some sense, the contact curvature radius is so small that it scales out of the problem, and we are thus left with geometrical lengths only. Due to strong adhesion, for example, the vesicle spreads out on the substrate as much as is allowed by the geometrical constraints which fix the enclosed area and the perimeter. Two length scales are involved: the vesicle size defined by $R = L/2\pi$, where L is the perimeter, and $R_{\rm s} = \sqrt{A/\pi}$ which is related to the enclosed area A. The ratio $R_{\rm s}/R$ can be referred to as the swelling factor: for a circle its value is unity, and it is smaller than unity otherwise. A more common definition of the swelling factor is

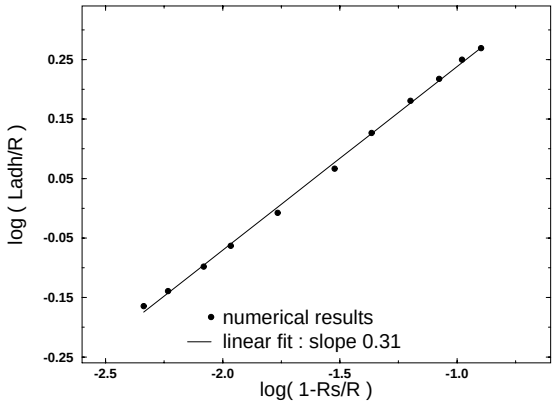

Fig. 4. The adhesion length as a function of the swelling factor.

$\tau \equiv A/\pi R^2$ (or $V/(4\pi R^3/3)$ in three dimensions), $\tau = 1$ for a circle and $\tau < 1$ otherwise. We shall however refer to $R_\mathrm{s}/R = \sqrt{A/\pi R^2}$ (which is the square root of the usual swelling factor) as the swelling factor in this paper.

Equilibrium (see Eq. (10)) imposes the following relation

$$\kappa \left(\frac{\partial^2 c}{\partial s^2} + \frac{c^3}{2} \right) \mathbf{n} + \frac{\partial \zeta}{\partial s} \mathbf{t} - c\zeta \mathbf{n} - \left(c\, w(\mathbf{r}) + \frac{\partial w(\mathbf{r})}{\partial \mathbf{n}} \right) \mathbf{n} = p\mathbf{n}\,. \tag{12}$$

Here p is the uniform hydrostatic pressure and the l.h.s. is the membrane force obtained from equation (10). In the limit where rigidity is small, curvature forces can be ignored to leading order. Additionally, for the free part of the vesicle (the part which is not in contact with the substrate) the adhesion potential can be neglected. For this part equation (12) simplifies to $p + c\zeta = 0$ (for the normal component) and $\partial\zeta/\partial s = 0$ (for the tangential one). As the membrane is stretched by the adhesion forces, the uniform tension ζ is non zero, and it fixes the radius of curvature of the free part which is a truncated circle. The vesicle morphology is thus entirely determined by R and R_s, and in the limit $R_\mathrm{s}/R \to 1$ and $d_0 \to 0$, L_adh obeys the following law:

$$L_\mathrm{adh} \sim R\,(1 - R_\mathrm{s}/R)^{\frac{1}{3}}\,. \tag{13}$$

There is a good agreement with the full numerical results (see Figs. 4, 5).

3.1.2 The flask regime, $R_c \sim R$

This regime is achieved for a very weak adhesion, large rigidity or a small vesicle. Of course the swelling factor must not be too close to 1. We expect the effect of rigidity to cause a decrease of the adhesion length for a given value of R and R_s. On the substrate, a vesicle gains adhesion energy at the price of curvature energy (see Fig. 6). The adhesion length follows then from a compromise between these two antagonist effects.

The adhesion energy gain is given obviously by

$$\Delta E_\mathrm{w} \sim w_0 L_\mathrm{adh}\,. \tag{14}$$

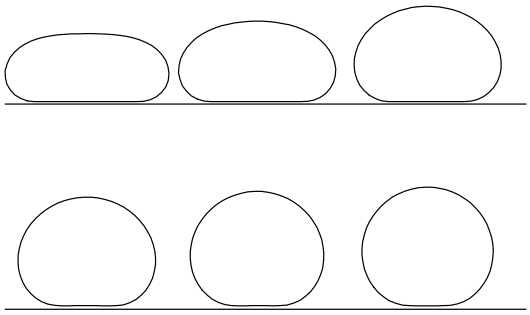

Fig. 5. Vesicle shapes corresponding to the swelling factor range shown in Figure 4.

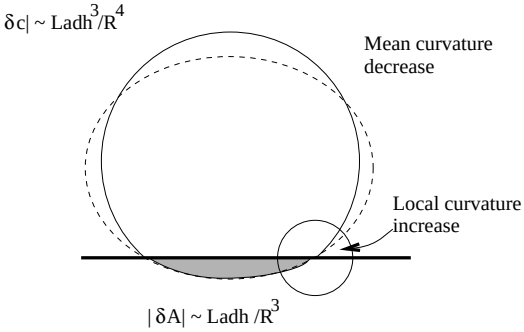

Fig. 6. During transformation between its free state (dashed line) and its adhering state (full line) the vesicle adhesion energy decreases, whereas its curvature energy increases. The liquid represented by the grey area must be redistributed elsewhere.

The curvature energy variation ΔE_c is, with $\delta c(s)$ the curvature difference between the final state (adhered) and the initial one (free):

$$\begin{aligned} \Delta E_\mathrm{c} &= \frac{\kappa}{2} \left(\int (c + \delta c)^2 \,\mathrm{d}s - \int c^2 \,\mathrm{d}s \right) \\ &= \frac{\kappa}{2} \left(\int 2c\delta c \,\mathrm{d}s + \int \delta c^2 \,\mathrm{d}s \right)\,. \end{aligned} \tag{15}$$

For vesicles that have swelled by a large enough amount ($R_\mathrm{s} \sim R$) the free curvature remains close to the constant value $c = 1/R$ and $\int c\delta c \,\mathrm{d}s \sim c \int \delta c \,\mathrm{d}s$. The length conservation implies $\int \delta c \,\mathrm{d}s = 0$, making this term negligible. The energy variation is thus quadratic with δc:

$$\Delta E_\mathrm{c} \sim \frac{\kappa}{2} \int \delta c^2 \,\mathrm{d}s. \tag{16}$$

The area conservation provides us with δc. The liquid represented by the grey area in Figure 6, must be redistributed elsewhere in the adhesion process. This area, δA, is computed as a small part of a disc with a basis L_adh and a radius R. With θ the angle so that $\sin(\theta/2) = L_\mathrm{adh}/2R$, we get, for a small adhesion length:

$$\delta A \sim \theta R^2/2 - L_\mathrm{adh} R \cos(\theta/2) \sim L_\mathrm{adh}^3/R\,. \tag{17}$$

The area redistribution produces a mean radius increase of the order of $\delta R \sim \delta A/R \sim L_\mathrm{adh}^3/R^2$. The decrease of

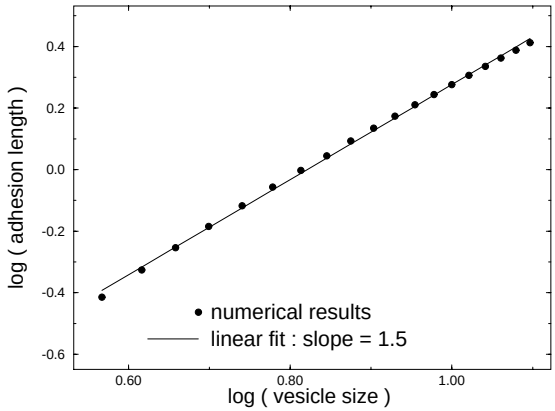

Fig. 7. Adhesion length variation with the vesicle size. Rigidity, swelling and adhesion are kept fixed.

curvature in the free part of the curve, $\delta c = -\delta R/R^2 \sim -L_{\rm adh}^3/R^4$, is compensated by a strong curvature increase around the contact point, ensuring $\int \delta c \sim 0$. Equation (16) thus entails

$$\Delta E_{\rm c} \sim \kappa R \delta c^2 \sim \kappa\, L_{\rm adh}^6/R^7\,. \tag{18}$$

Equating the two variations (14) and (18), we obtain

$$L_{\rm adh} \sim \left(\frac{w_0}{\kappa}\right)^{\frac{1}{5}} R^{\frac{7}{5}}\,. \tag{19}$$

The full numerical result provides a good agreement with the above law (see Fig. 7).

Note that in this regime, the adhesion length increases faster than the size, with an effective power law $L_{\rm adh} \sim R(R/R_{\rm c})^{2/5}$.

3.1.3 Extension of the analytical results to 3D

The above analysis can be extended to $3D$ in a straightforward manner. The area variation δA becomes a volume $\delta v \sim L_{\rm adh}^4/R$ from which we get the curvature variation $\delta c \sim L_{\rm adh}^4/R^5$, with $L_{\rm adh}$ the radius of the adhered part. The loss of curvature energy, $\delta E_{\rm c}^{3D} \sim \kappa \delta c^2 R^2$, counterbalances the gain due to adhesion, $\delta E_{\rm w}^{3D} \sim L_{\rm adh}^2 w_0$, leading to:

$$\kappa \left(\frac{L_{\rm adh}^4}{R^5}\right)^2 R^2 \sim L_{\rm adh}^2 w_0\,, \tag{20}$$

implying that

$$L_{\rm adh}^{3D} \sim R^{4/3} \left(\frac{w_0}{\kappa}\right)^{1/6}. \tag{21}$$

3.2 The Lagrange multiplier

We complete the equilibrium analysis by addressing the question of the Lagrange multiplier ζ. We shall distinguish between a strong enough adhesion (the tense regime) and a weak adhesion.

3.2.1 The strong adhesion regime

As we have seen before this regime corresponds to a shape which is a truncated circle and the total energy can be approximately written as

$$E \sim \zeta L + pA - w_0 L_{\rm adh}\,. \tag{22}$$

Here the variational parameters are L and A. The pressure p is the hydrostatic pressure, so E is rather an enthalpy than an energy. A large perimeter for a given enclosed surface would favor spreading thanks to adhesion. This leads thus to a positive tension, acting against the membrane extension. The Lagrange multiplier ζ and the hydrostatic pressure p ensure that the desired perimeter and area act in a way to render minimum the energy, so that:

$$\left(\frac{\partial E}{\partial L}\right)_A = -w_0 \left(\frac{\partial L_{\rm adh}}{\partial L}\right)_A + \zeta = 0$$
$$\left(\frac{\partial E}{\partial A}\right)_L = -w_0 \left(\frac{\partial L_{\rm adh}}{\partial A}\right)_L + p = 0\,.$$

To first order in the small parameter $1 - R_{\rm s}/R$, we get, by using equation (13):

$$\zeta \sim w_0 \left(1 - \frac{R_{\rm s}}{R}\right)^{-2/3}, \qquad p \sim -\zeta/R\,. \tag{23}$$

3.2.2 The weak adhesion regime

This limit means that curvature forces are large enough. In contrast to adhesion forces, these forces tend to decrease the perimeter (and increase the area) causing the shape to tend towards a circular shape. In the limit of small vesicles, the tension is dominated by the rigidity contribution and is therefore negative. For an intermediate size of the vesicle, the rigidity and the adhesion compete and one must find the tension from an interplay between these effects. The full expression for the energy is:

$$E = pA + \zeta L - w_0 L_{\rm adh} + \frac{\kappa}{2}\int c^2 {\rm d}s\,. \tag{24}$$

The rigidity enters here both in the adhesion length (see Eq. (19)) and explicitly in the Helfrich energy.

Minimization, with a constant swelling factor τ, yields

$$\left(\frac{\partial E}{\partial L}\right)_\tau = -w_0 \left(\frac{\partial L_{\rm adh}}{\partial L}\right)_\tau + \zeta + p\left(\frac{\partial A}{\partial L}\right)_\tau + \frac{\kappa}{2}\frac{\partial}{\partial L}\int c^2 {\rm d}s\Bigg)_\tau = 0\,. \tag{25}$$

Assuming again $p \sim -\zeta/R$, which is here an approximated value, we get

$$\zeta \sim \left[w_0 \left(\frac{\partial L_{\rm adh}}{\partial L}\right)_\tau - \frac{\kappa}{2}\frac{\partial}{\partial L}\int c^2 {\rm d}s\right)_\tau\right](1 - R_{\rm s}/R)^{-1}. \tag{26}$$

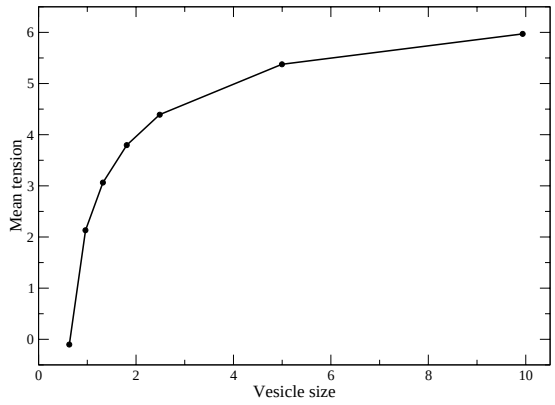

Fig. 8. Membrane tension as a function of the vesicle size. numerical values: $R = 0.5 \to 10$, $R_s/R = 0.96$, $R_c = 0.4$, $d_0 = 0.06$, $w_0 = 2.5$.

Both adhesion and curvature energy increase more rapidly than linearly with R in the weak adhesion regime (see (19) and its determination), while they scale linearly with the size in the tense regime. Thus the tension increases with R and saturates to a limiting value for large vesicles (see Fig. 8).

4 Dynamics: hydrodynamics dissipation

On the vesicle scale ($R \sim 10$ μm) and for the expected velocities ($V \sim 1$ μm/s), dynamics are completely dominated by dissipative processes. The energy injected is instantaneously dissipated in the various degrees of freedom. Local dissipation due to molecular reorganization, characterized by the Leslie coefficient, is negligible in comparison to hydrodynamics modes [29]. Additionally, as specified above, we restrict ourselves to non-dissipative adhesion. Hydrodynamics dissipation is therefore taken to be as the dominant process. Hydrodynamics dissipation occurs in the bulk fluid as well as within the membrane. We provide below an estimate on the conditions under which dissipation within the membrane may be disregarded.

Let us first consider the dissipation arising from a velocity gradient along the membrane. The velocity continuity implies that these gradients are of the same order of magnitude as the bulk velocity gradients. So, the internal and external dissipations, given by η (or η_m) $\int (\nabla v)^2 \mathrm{d}\tau$, are given respectively by:

$$D_{\rm int} \sim \eta_{\rm m} (V/R)^2 h R^2 \sim \eta_{\rm m} V^2 h \,, \tag{27}$$

$$D_{\rm ext} \sim \eta (V/R)^2 R^3 \sim \eta V^2 R \,, \tag{28}$$

with η_m the membrane viscosity and h its thickness. As long as $\eta R/\eta_m h \gg 1$ the condition $D_{\rm ext} \gg D_{\rm int}$ is satisfied. Yeung and Evans measured a ratio $\eta_m/\eta \sim 100$ leading to a critical radius of the order of 100 h ~ 1 μm for the cross-over [31,32].

In the same way, we can check the influence of the dissipation due to a relative sliding of the two monolayers. The tangential stress continuity at the membrane/liquid interface implies

$$\eta \frac{V}{R} \sim \eta_{\rm m} \frac{\delta V}{h} \,, \tag{29}$$

with δV the relative velocity of the two monolayers. From these, we deduce the internal and external dissipations:

$$D_{\rm int} \sim \eta_{\rm m} (\delta V/h)^2 h R^2 \sim (\eta V^2 R) \frac{\eta}{\eta_{\rm m}} \frac{h}{R} \,, \tag{30}$$

$$D_{\rm ext} \sim \eta (V/R)^2 R^3 \sim \eta V^2 R \,, \tag{31}$$

leading to the condition $\eta h/\eta_m R \ll 1$, which is always fulfilled.

That is to say, as long as the vesicle size is large in comparison to 1 μm (a situation encountered for most practical purposes in experiments with liposomes), dissipation due to the membrane viscosity is negligible. Additionally, the velocity discontinuity δV across the membrane is negligible (see Eq. (29)).

Having shown that dissipation is dominated by bulk effects, we are in a position to write down the basic governing equations. Inertia are small (the small Reynolds number limit). The velocity field obeys the Stokes equations:

$$\begin{aligned} \eta \Delta \mathbf{v} - \nabla p &= 0 \\ \nabla . \mathbf{v} &= 0 \,. \end{aligned} \tag{32}$$

The main difficulty arises from the fact that the boundary is unknown *a priori* (free boundary). Thanks to the linearity of the Stokes equations, the velocity field in the bulk can be integrated out by means of the Green's function. We thus end up with an evolution equation of the contour only, at the price of nonlocality.

4.1 Boundary conditions

Let $\mathbf{v}^-$, $\mathbf{v}^+$ designate the fluid velocities close to the membrane, but outside the vesicle, and inside, respectively. Let $\mathbf{v}^{\rm m}$ be the membrane velocity. We assume that the two monolayers form a unique entity. As we saw above, the sliding motion between the monolayers is negligible (see Eq. (29)). The non slip condition implies the equality between the tangential components of the above defined three velocities,

$$v_{\rm t}^- = v_{\rm t}^+ = v_{\rm t}^{\rm m} . \tag{33}$$

On the other hand, mass conservation across the bilayer leads to

$$v_{\rm n}^- = v_{\rm n}^+ = v_{\rm n}^{\rm f} \tag{34}$$

with $v_{\rm n}^{\rm f}$ the fluid normal velocity. The vesicle impermeability provides the last relation $v_{\rm n}^{\rm f} = v_{\rm n}^{\rm m}$. The fluid velocity is thus continuous across the membrane, and is equal to the membrane velocity.

Finally, the non slip condition entails that $\mathbf{v}$ vanishes at the substrate. Nevertheless a sliding motion of the vesicle is allowed due to the fact that the distance between the vesicle and the substrate is not exactly zero. That is to say, we allow for a thin fluid layer between the substrate and the membrane. Experimental studies on vesicles have reported that under a weak enough adhesion, there is always a gap (of the order of 50−100 nm) between the substrate and the vesicle [33].

4.2 Green's function

The Stokes equations are linear and can be rewritten in an integral form over the boundaries (the vesicle and the substrate) by using Green's function techniques. The main idea is to express the velocity field as the superposition of elementary fields, each one being the response to an external point force $\mathbf{f}$ applied on the fluid (see Fig. 10). We shall assume that there is no viscosity contrast between inside and outside. The same hydrodynamical equations thus hold in the whole aqueous medium and the expected expression for the velocity is formally given by $\mathbf{v} = \int G\mathbf{f}\mathrm{d}s$. The membrane is a location of forces $\mathbf{f}_{\mathrm{memb}}$, that counterbalances the forces associated with the velocity field.

The Green's function for the velocities, denoted by G, has been introduced by Oseen and is often referred to as the Oseen tensor [34]. Note that because G is the response function to a vector field, it is a tensor (the shear and the normal stresses are different). G is a solution of the following system (with the summation convention on repeated indices):

$$\begin{aligned} &\eta\,\partial_{kk}G_{ij}(\mathbf{r},\mathbf{r}') - \partial_i P_j(\mathbf{r},\mathbf{r}') + \delta(\mathbf{r}-\mathbf{r}')\mathbf{u_j} = 0 \\ &\partial_i G_{ij}(\mathbf{r},\mathbf{r}') = 0\,. \end{aligned} \tag{35}$$

The vector $\mathbf{P}$ is the Green's function for the pressure field, which plays no role in the final integral formulation, so that we have not felt it worthwhile to specify it. Note that the above Green's function is the free space one (that is no boundary condition has to be specified if the velocity vanish at infinity). A Green's function for a half space is known [35], and we could make use of it. In that case the boundary condition at the substrate would have been satisfied automatically. A particular advantage for using the free space propagator lies in the fact that it can be adopted to any wall geometry (*e.g.* a roughness which is always present in real situations...), or simply if one wishes to introduce a second wall (vesicles in a channel). The direct calculation of the Green's function and the derivation of the integral equation can be found in [16]. We shall thus only give the results here. Let us set for brevity $r \equiv |\mathbf{r}-\mathbf{r}'|$ and r_i the i^{th} component of the vector $\mathbf{r}-\mathbf{r}'$, G is given in 2D by:

$$G_{ij} = \frac{1}{4\pi\eta}\left(-\delta_{ij}\ln(r) + \frac{r_i r_j}{r^2}\right)\cdot \tag{36}$$

Figure 9 illustrates the behavior of the Green's function. This function diverges logarithmically for $r = 0$ and $r \to \infty$. The first divergence is integrable. The divergence at long distance deserves a special attention, as it will be dealt with later in this paper. Additionally, G must contain a special cut-off. Another way of saying the same thing is that the argument of ln must be dimensionless. Let the spatial cut-off be denoted by U_r. We must then have $\log(r/U_r) = \log(r) - \log(U_r)$. As shown below, the Oseen tensor only enters the expression $\int G\mathbf{f}\mathrm{d}s$. The total force $\int \mathbf{f}$ on a fluid element is zero in the Stokes limit; the additive constant does not matter.

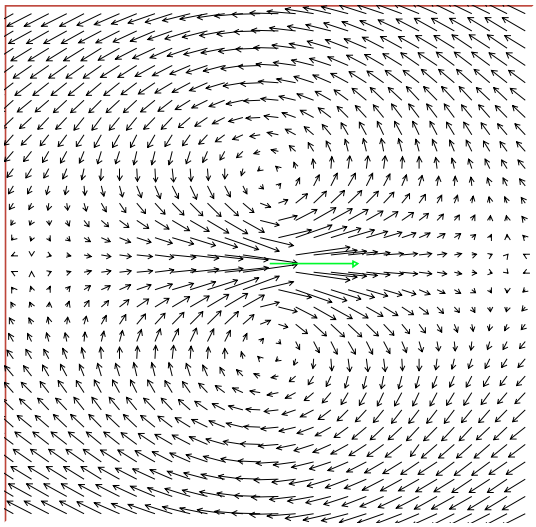

Fig. 9. Green's function associated to a point force oriented along $\hat{\mathbf{x}}$.

4.3 Integral equation

The velocity field at a given point in the fluid obeys the following equation [16]:

$$\mathbf{v}(\mathbf{r}) = \int_{\Gamma} \mathrm{d}\tau\, G(\mathbf{r}-\mathbf{r}')\,\mathbf{f}(\mathbf{r}')\,. \tag{37}$$

Here $\mathbf{r}'$ corresponds to the force sources localized on two boundaries: the vesicle boundary Γ_{v} and the substrate one, Γ_{s}. From the very definition of the stress tensor, $\sigma_{ij} = -p\delta_{ij} + \eta(\partial_j v_i + \partial_i v_j)$, it is a simple matter to see that the total force (per unit area) from the substrate (the reaction force) is given by

$$\mathbf{f}_{\mathrm{sub}} = p\,\hat{\mathbf{y}} - \eta\frac{\partial v_x}{\partial y}\,\hat{\mathbf{x}}\,. \tag{38}$$

The reaction force of the membrane is given by (10). The velocity field takes the following final form

$$\begin{aligned} \mathbf{v}(\mathbf{r}) = &\int_{\Gamma_{\mathrm{v}}} G(\mathbf{r}-\mathbf{r}')\mathbf{f}(\mathbf{r}')_{\mathrm{memb}}\,\mathrm{d}s' \\ &+ \int_{\Gamma_{\mathrm{s}}} G(\mathbf{r}-\mathbf{x}')\left(p(x')\,\hat{\mathbf{y}} - \eta\frac{\partial v_x}{\partial y}(x')\,\hat{\mathbf{x}}\right)\mathrm{d}x'. \end{aligned} \tag{39}$$

The various terms involved in $\mathbf{f}_{\mathrm{memb}}$ depend only on the membrane geometry, except the "tension", which will be discussed later. The second force, arising from the wall, is *a priori* unknown, and must be evaluated self consistently, using the condition that the velocity vanishes on the substrate.

Equation (39) is valid everywhere in the fluid. Taking the limit $\mathbf{r} = \mathbf{r_m}$ where $\mathbf{r_m}$ is the membrane position we obtain the membrane velocity, and thus dynamics can be determined starting from some initial condition. As mentioned before, the fluid velocity field is integrated out, and dynamics is described by the knowledge of the contours contribution; this is done at the price of nonlocality.

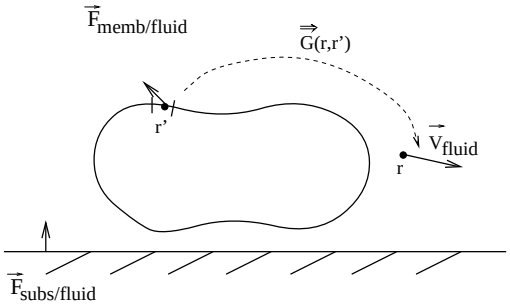

Fig. 10. The Oseen tensor G is here defined as the velocity field response to a point force in an infinite fluid at rest at infinity. It provides a relation, between two vectors, the velocity and the force; and two locations $\mathbf{r}$, where the velocity is observed, $\mathbf{r}'$, where the force is applied.

4.4 The 2D logarithmic divergence

The logarithmic divergence at long distance is a problem which is specific to the 2D character. For this reason the evaluation of the Stokes law (the drag force), for example, is ill-posed and one has to resort to the Oseen approximation [36] in order to cure this pathological behavior. The crux of the Oseen approximation is based on the fact that though inertia effects are small in principle, they play a role at long distance. Nevertheless, for an adhering vesicle, it turns out that the *local viscous dissipation* due to the small distance between vesicle and substrate dominates the dynamics, and this sets a short length cut-off. Let us be more specific and estimate the viscous and inertial forces acting on a cylinder, as a function of the distance to a wall. This will allow us to specify the validity of the Stokes equations in 2D.

The purely viscous friction acting on a cylinder which is moving at velocity V at distance d from the wall and having a radius R is given by [37]:

$$F_{\rm visq} = 4\pi\eta V \frac{1}{\ln(1+d/R+\sqrt{(d/R)^2+2d/R})} \sim \frac{4\pi\eta V}{\sqrt{2d/R}}. \tag{40}$$

The second equality in equation (40) corresponds to the asymptotic case of interest, $d \to 0$. As expected, this force becomes logarithmically small as d increases, and thus inertia may become important.

The inertial force acting on a cylinder moving with velocity V in an unbounded fluid is, to leading order in Re,

$$F_{\rm iner} = 4\pi\eta V \frac{1}{1/2 - C - \ln \mathrm{Re}} \sim \frac{-4\pi\eta V}{\ln \mathrm{Re}}. \tag{41}$$

$F_{\rm iner}$ goes to zero when the Reynolds number vanishes, and is thus intrinsically related to fluid inertia. Assuming this expression to hold (in an order of magnitude sense) close enough to a substrate, we find that the validity for the Stokes equation, $F_{\rm visq} \gg F_{\rm iner}$, becomes:

$$\sqrt{d/R} \ll |\ln \mathrm{Re}|\,. \tag{42}$$

Typically, Re is at most of the order of Re $\sim 10^{-3}$ and $d/R < 0.1$. Therefore, disregarding inertia is justified beyond any doubt, despite the 2D specificity of the problem. This means, as anticipated above, that a short distance cut-off prevails over the Oseen correction which usually cures the ill-posedness of the Stokes problem. It must be mentioned, however, that the behavior of the velocity field at long distances should need a special treatment, a question in which we are not interested in this paper.

5 The numerical scheme

In principle, given an initial condition, we can determine the velocity field. Then each point is moved in the normal direction by a quantity $v_{\rm n}\delta t$, and so on. By this procedure we can study vesicle dynamics in the course of time. The initial condition can be specified in terms of the coordinates $(x,y)_i$, i being the index associated to the $N \sim 100$ discretisation points along the membrane. The numerical code will provide the evolution law for these N points. Of course the mesh size on the membrane must remain small in comparison to the distance d_0 from the substrate. We use an inhomogeneous discretisation, which is taken to be finer close to the substrate.

The substrate discretisation is typically performed with $N_2 \sim 100$ points indexed by j. Under the vesicle the mesh is chosen to be smaller but close to d_0, whereas far away from the adhered part, we have used a mesh size on the substrate which varies as j^2. We explored domains of typical sizes equal to $10R$ on both sides of the vesicle.

The procedure can be summarized in the following three main steps: (a) computation of the membrane forces $\mathbf{f}_i$, using equation (10) (the determination of ζ is discussed below); (b) evaluation of the wall reaction, by taking advantage of the non slip condition on the substrate. This information, coupled with the velocity expression (39), amount to inverting the integral equation. This means that we invert a $2N_2 \times 2N_2$ matrix. The $2N_2$ unknown parameters are $p_{j'}$ and $\partial v_x/\partial y)_{j'}$. The discretized version of the integral equation to be inverted is

$$\mathbf{v}_j = 0 = \sum_i G(\mathbf{x}_j - \mathbf{r}_i)\,\mathbf{f}_i\,ds_i + \sum_{j'} G(\mathbf{x}_j - \mathbf{x}_{j'})\,\left(p(x_{j'})\,\hat{\mathbf{y}} - \eta\frac{\partial v_x}{\partial y}(x_{j'})\,\hat{\mathbf{x}}\right)\,dx_{j'}. \tag{43}$$

The inversion yields the $p_{j'}$ and $\partial v_x/\partial y)_{j'}$ values; the third step, (c) consists of computing the membrane velocity by using (39). Once the velocity is obtained, the displacement of each membrane point is, in principle, straightforward. The time discretisation used in this last step is such that $\mathrm{d}t < \mathrm{d}s^n$, with n the highest order of the spatial derivative. This is set by the Helfrich force, which contains a fourth order derivative, and in principle, $n = 4$. This imposes a rather drastic small time step $\mathrm{d}t \sim 10^{-4}$ for a reasonable mesh size of 10^{-1} [38]. It will be an important task for future investigations to make use of more sophisticated temporal schemes with the aim of reducing the computing time. In fact in 2D the vesicle acquires a permanent regime within 10 to 30 minutes on the fastest commercial

PC's. In 3D there is a strong need for optimizing the code if one wishes to access to a full quantitative study, as it has been done for similar situations in [7,10]. These codes should allow for an extensive future simulation.

5.1 Dealing with the constraints

The Lagrange multiplier (ζ is the Lagrange multiplier) formalism is the traditional way for fixing constraints. Once the velocity field expression has been obtained formally (39), the value of ζ can be determined from the constraint equation of incompressibility $v_{\rm n}c + \partial v_t/\partial s = 0$. This set of equations involves ζ through the velocities (39), expressed as integral functions of the membrane forces (10), which themselves depend on ζ. ζ can then be obtained by inverting an integral equation. We found it more convenient to treat this part in a different manner, which is more straightforward. We imagine that two neighboring material points (which are taken to be identical to the discretisation points) on the membrane are coupled to each other by a "stiff spring". In other words, we penalize any deviation ds_i between two discretisation points on the membrane, by adding in the forces a spring-like term $\zeta^s = K\,(ds_i - ds_{0,i})$, with $ds_{0,i}$ a reference value, and K is taken large enough in order to keep ds_i as close as possible to $ds_{0,i}$. With this prescription the length is conserved within less than 1%. Note that in this formulation, the tension is explicitly expressed in terms of the membrane geometry. In some sense, with the "Lagrange multiplier approach", ζ adapts itself instantaneously to other forces in order to keep the local length ds_i unchanged, whereas with the "spring model", ζ^s adapts itself adiabatically, albeit with an internal time scale (but short in comparison to the relaxation time towards the desired dynamics).

The volume constraint (area constraint in 2D) is *a priori* ensured by the dynamical equation "div $\mathbf{v} = 0$", implicitly involved in the Green's function expression. At long enough time a "drift" of the enclosed area may be noticed, due to numerical errors. In order to circumvent this difficulty, we have introduced an effective external pressure $p = K'(A - A_0)$ in the numerical code, enforcing the area to the desired value A_0. Once the value of the constant K' is adjusted, the area is practically constant.

6 Out of equilibrium scaling laws

The computation method proposed above is quite general and may be used for diverse situations. We shall confine ourselves here to the case where motion is due to an adhesion gradient (haptotaxis). In principle, as the vesicle moves the adhesion potential increases in absolute value, and this should lead to a continuous flattening of the vesicle. In biological situations the potential is regulated so that on the average it remains constant in the frame of the cells. We shall thus assume that the adhesion energy is constant in the vesicle frame and write the adhesion potential as in (3). Because $\bar{w} = w_0 + (x - x_{\rm m})\delta w$, the adhesion under the vesicle, where $x = x_{\rm m}$, is permanently equal w_0. However, the vesicle evolves permanently in a gradient. The driving force F (per unit length in the z direction) is the adhesion difference δw_0 between upstream and downstream contact points

$$F = \delta w_0 = L_{\rm adh}\,\nabla \bar{w}\,. \tag{44}$$

After transients have decayed, the vesicle adopts a stationary behavior that will be discussed in the next sections. We shall develop an analytical theory based on heuristic arguments which capture the essential features found in the full numerical analysis.

6.1 Membrane morphology

6.1.1 Characteristic times

It will be interesting to compare the time associated with the driving force, with that involved in the relaxation of the shape of the vesicle as if it were free. The first time is obtained by combining the viscosity with the energy (per unit length) causing the vesicle motion. That energy is typically of order $E = F\,R = \delta w_0 R$. The energy per unit volume is thus $E_{\rm vol} = \delta w_0/R$. The corresponding time scale τ_1, is

$$\tau_1 \sim \eta R/\delta w_0 \sim 10^{-2}\ {\rm s}\,. \tag{45}$$

The other time scale corresponds to relaxation at equilibrium and may be estimated as [29] (which is a purely dimensional consequence):

$$\tau_2 \sim \eta\, R^3/\kappa \sim 1\ {\rm s}\,. \tag{46}$$

One sees that the time scale associated with adhesion is much faster. We may ask the question of by how much the non-equilibrium shape would be different from the equilibrium one?

6.1.2 Stationary shape

We take as a reference value for the equilibrium contact curvature $c_0 = \sqrt{2w_0/\kappa}$ corresponding to a homogeneous substrate of the same mean adhesion w_0. We may estimate the deviation from the equilibrium shape by evaluating the contact curvatures on both sides of the vesicle. The non equilibrium contact curvature is a combination of two effects: the adhesion, and the hydrodynamical pressure. The driving force is the adhesion gradient. The pressure distribution produces a drag force slowing down the motion. So, an overpressure ahead of the vesicle tends to decrease the contact curvature (whereas an underpressure decreases it at the rear). This effect is typically given by [8]

$$\frac{\delta c}{c_0} \sim \frac{\eta V}{w_0 (d_0 c_0)^{\frac{1}{2}}}\cdot \tag{47}$$

On the other hand, the adhesion is larger ahead of the vesicle and as a consequence, the curvature increases there by an amount

$$\frac{\delta c}{c_0} \sim \frac{\delta w_0}{2 w_0}\cdot \tag{48}$$

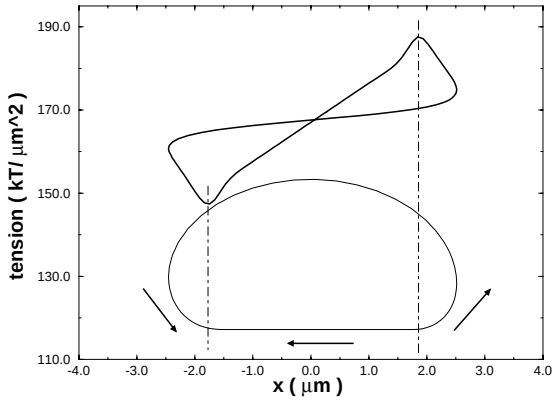

Fig. 11. Bottom: Morphology of a vesicle moving to the right. Top: Membrane tension as the function of the abscissa x; The part of the curve which is slowly increasing corresponds to the upper part of the membrane, far from the substrate, and the rest corresponds to the lower part. The dashed line show the correlation between the contact point positions and the tension extrema. Directions of the tangential hydrodynamics forces are represented by the three arrows.

The two corrections have opposite signs and turn out to be close to each other in absolute values for the set of parameters explored so far. Thus the upstream and downstream shapes are only slightly affected. Note that the hydrodynamical force and the adhesion one are interdependent. Indeed, the first one is proportional to the velocity which itself varies with δw_0. The presence of these two antagonist effects is specific to haptotaxis. Under a shear flow, for example, the vesicle morphology is on the contrary drastically modified leading to a hydrodynamical net lift force causing a complete unbinding from the substrate [8].

6.1.3 Out of equilibrium membrane tension

The hydrodynamical flow induces a tangential force along the membrane contour that must be counterbalanced by membrane forces. The only tangential component in the membrane force (10) arises from the tension gradient $\partial\zeta/\partial s$ (see Fig. 11). The mean tension value remains close to the equilibrium one, albeit it is inhomogeneous. Indeed, the adhesion gradient does not tend to change the global membrane area. Tangential hydrodynamics forces just compresse the membrane around the rear contact point and symmetrically extends it around the fore contact point, leading respectively to a smaller and a larger tension.

6.2 Analytical and numerical results for the translational velocity

6.2.1 Analytical approach

The following analysis can be made for any driving force F. The power associated with the driving force F is FV and is instantaneously dissipated in hydrodynamical modes. V represents the translational velocity of the vesicle. The law for the migration velocity is obtained from the relation $FV \sim D$, with D the viscous dissipation, which is the main quantity to be determined. The dissipation is given by $\eta(\nabla \mathbf{v})^2$ integrated over the volume in which dissipation is effective.

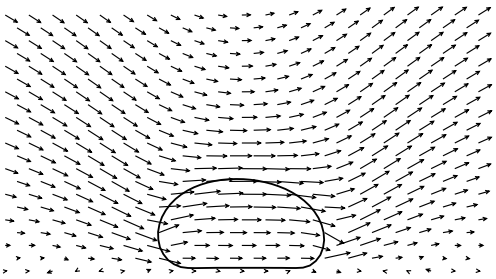

Fig. 12. Velocity field around the vesicle. Important velocities are observed at two places which are represented schematically on the next picture. The rolling motion of the vesicle induces expulsion of water at the front and pumping at the rear. As already discussed in Section 4.4, the velocity field behavior at long distance is irrelevant (see also remark [30]).

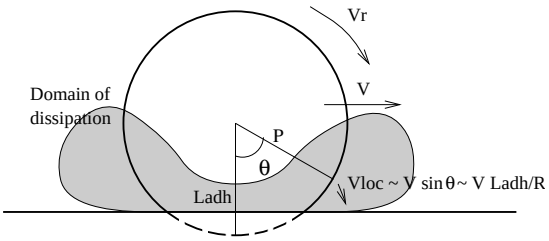

Fig. 13. Schematic representation of the main dissipation domain.

The most important velocity gradients are localized in a domain which is close to the contact points (see Fig. 12). This zone is represented schematically in grey in Figure 13. The penetration of disturbance of the velocity field in the bulk due to the presence of the vesicle is typically $L_{\rm adh}$. The local velocity in this domain, at a distance $L_{\rm adh}$ from the contact point is $V_{\rm loc} \sim V \sin\theta \sim V\, L_{\rm adh}/R$, with the angle θ defined in Figure 13. The velocity gradient is thus typically of order $V_{\rm loc}/L_{\rm adh}$, leading to $\nabla V_{\rm loc} \sim V_{\rm loc}/L_{\rm adh} \sim V/R$. Note that the result is obvious: on the global scale of the vesicle size R, the vesicle moves with velocity V, hence the induced gradients are of order V/R. Since the local velocity gradient extends over $L_{\rm adh}$, the effective "volume" (surface in 2D) in which dissipation occurs scales as $L_{\rm adh}^2$. The total dissipation is thus given by:

$$D \sim \eta L_{\rm adh}^2 \left(\frac{V}{R}\right)^2 . \tag{49}$$

Equating the dissipation with the injected power, we obtain the velocity law (with F a driving force per unit length):

$$V \sim \frac{F}{\eta}\left(\frac{R}{L_{\rm adh}}\right)^2 . \tag{50}$$

This law is in a good agreement with the numerical results presented below.

We must distinguish between two regimes discussed in Section 3: (i) the tense one where $L_{\rm adh} \sim R$, in which case the migration law given above becomes similar to the Stokes law in 2D far away from a wall (as stated before the Stokes law in 2D has logarithmic corrections). We also note that the law in question differs from that of a cylinder (Sect. 4) close to the wall. This difference will be discussed below. (ii) The flask regime, where $L_{\rm adh}$ is given by (19). It follows then that the velocity is given by

$$V \sim \frac{F}{\eta}\left(\frac{R_{\rm c}}{R}\right)^{4/5}. \tag{51}$$

6.2.2 The power law in 3D

We strongly expect the arguments used in the derivation of the velocity power law in 2D to remain valid in 3D. For a vesicle in a shear flow, the full 3D simulation has been recently performed [10]. It leads to results very similar to the 2D results, even if the shear flow induces a prolate/oblate transition, obviously not observable in 2D. This transition should not appear in haptotaxis. Indeed the adhesion potential favors the oblate shape and, in contrast with the previous situation, no hydrodynamical effect tends to induce a prolate shape. Of course the geometrical constraints on volume and area in 3D are much less restrictive than the constraint on area and perimeter in 2D. Complex velocity fields on the membrane itself are especially expected in 3D with no equivalence in 2D. Nevertheless, the characteristic length R and the equilibrium radius of curvature $R_{\rm c}$ remain robust and well defined in 3D and play similar roles in the dissipative processes. For our purpose, the only difference is thus that the effective volume of dissipation is $L_{\rm adh}^3$ and the local velocity gradient remains proportional to V/R. We obtain the following dissipation rate:

$$D \sim \eta L_{\rm adh}^3 \left(\frac{V}{R}\right)^2, \tag{52}$$

leading to the velocity scaling law:

$$V \sim \eta \frac{F}{R}\left(\frac{R}{L_{\rm adh}}\right)^3. \tag{53}$$

Using the scaling law $L_{\rm adh} \sim R^{4/3} R_{\rm c}^{-1/3}$ (Eq. (21)) for the adhesion radius in the small adhesion regime, we obtain the following relation for the velocity:

$$V \sim \eta \frac{F R_{\rm c}}{R^2}. \tag{54}$$

The Stokes law for a sphere moving in a viscous fluid is $V \sim \eta F/R$, and remains valid close to a wall up to logarithmic corrections [39]. The new power law $1/R^2$ is intrinsically related to the vesicle deformability and to its ability to spread on the substrate. This deviation from the Stokes law is strong enough and is thus not devoid of experimental testability.

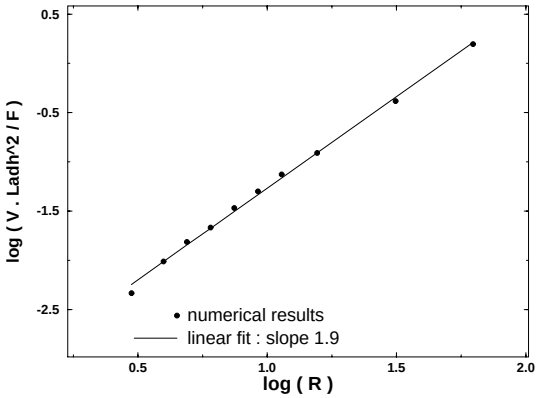

Fig. 14. Variation of the vesicle size R. The ratio $R_{\rm s}/R$ is kept fixed. (Numerical values: $R = 0.5 \rightarrow 10$, $Rs/R = 0.96$, $R_{\rm c} = 0.4$, $d_0 = 0.06$.)

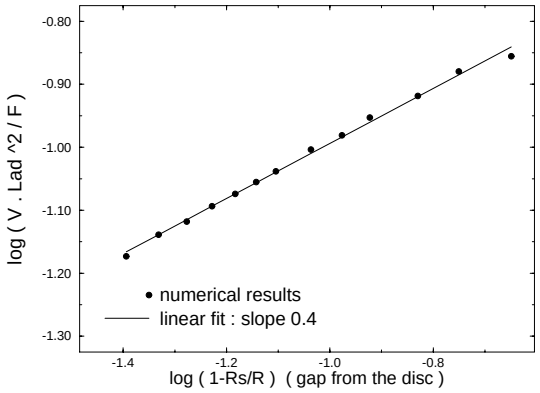

Fig. 15. Variation of the reduced volume. (Numerical values: $Rs/R = 0.78 \rightarrow 0.95$, $R = 1.1$, $R_{\rm c} = 0.5$, $d_0 = 0.06$.)

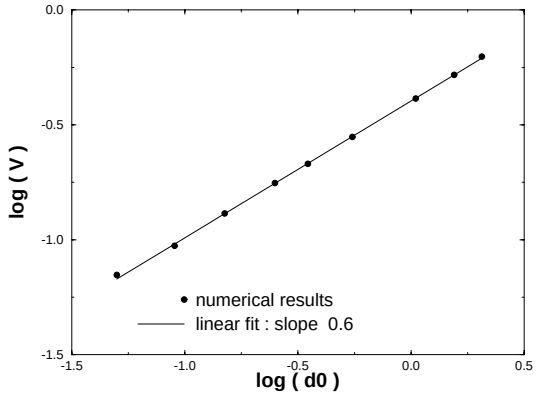

Fig. 16. Variation of the potential range. (Numerical values: $Rs/R = 0.88$, $R = 1.1$, $R_{\rm c} = 0.6$, $d_0 = 0.05 \rightarrow 2$.)

6.2.3 Numerical determination of the translational velocity

We explored numerically the parameter space (R, $R_{\rm s}$ and $R_{\rm c}$) (recall that $R_{\rm s}$ is proportional to the square root of the enclosed area; see Sect. 3). The results are presented in Figures 14, 15 and 16. In the analytical analysis above we have made our reasoning for a given swelling factor, and in addition we did not evoke the lubricated film beneath. Dimensionally R and $R_{\rm s}$ are the same, but their

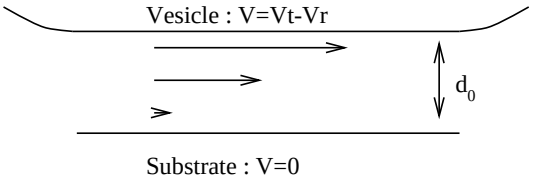

Fig. 17. Schematic view of the different velocities.

ratio fixes the swelling and it is of great importance to analyze its effect. The numerical part allows one to determine the dependence of the migration velocity as a function of these quantities, and thus a complete analysis can be achieved.

We have confronted our analytical results with the numerical ones and one arrives to the conclusion that the migration velocity (in 2D) takes the following form

$$V \sim \frac{F}{\eta}\left(\frac{R}{L_{\rm adh}}\right)^2 \sqrt{\frac{d_0}{R_{\rm c}}}\left(1-\frac{R_{\rm s}}{R}\right)^{0.4}. \qquad (55)$$

The exponents are determined within ± 0.1 accuracy. The first factor of this law is the analytical prediction (51). The third factor contains the swelling effect. For an increasing vesicle area, we found that the velocity varies approximately as $(1-R_{\rm s}/R)^{0.4}/L_{\rm adh}^2$ (see Fig. 15). In fact the numerator accounts for a direct swelling effect: the larger is the swelling the smaller is the velocity. Indeed a larger swelling corresponds to a greater volume and thus to a stronger dissipation. The denominator contains $L_{\rm adh}^2$ and this term creates an antagonist effect. Indeed the higher is the swelling the smaller is the adhesion area (for a sphere that area goes to zero). We have seen before that in the tense regime $L_{\rm adh}$ varies in 2D as $(1-R_{\rm s}/R)^{1/3}$ (see Eq. (13)). Thus the denominator variation dominates entailing, amazingly, that the velocity decreases when the vesicle total area increases, for a given driving force.

Finally the factor $\sqrt{d_0/R_{\rm c}}$ in (55) is valid in the small adhesion regime (the only regime explored numerically). In the limit of vanishing $R_{\rm c}$ (strong adhesion or small rigidity) the velocity should become independent of $R_{\rm c}$ (which must scale out of the problem). Thus the divergent term $R_{\rm c}^{-0.5}$ is not relevant and we suggest that it must be substituted by $R^{-0.5}$ (R is the only length scale we are left with). In this way our result would agree with the solution of cylinder close to a wall (Eq. (40)). So far, exploring numerically the cross-over to the tense regime has proven to be difficult.

6.3 Analytical and numerical results for the rotational velocity

6.3.1 Analytical scaling law

The sliding ratio $\tau_{\rm s} = 1 - V_{\rm r}/V$ (where $V_{\rm r}$ is the rotation velocity) is governed by an interplay between dissipation in the fluid gap between the membrane and the substrate, and the dissipation around the vesicle. For a vanishingly small gap, we expect $\tau_{\rm s} \to 0$. On the other hand, far from the wall a purely sliding motion minimizes the dissipation and $\tau_{\rm s} = 1$. The question is how does sliding vanish by decreasing the gap, whose width is given by d_0. In order to estimate $\tau_{\rm s}$, we assume that dissipated powers under the vesicle and that on the global scale of the vesicle have a given ratio. That means that the rotational velocity adapts itself in order to keep the two dissipations in the same ratio when the size changes. This condition ensures a global stationary motion.

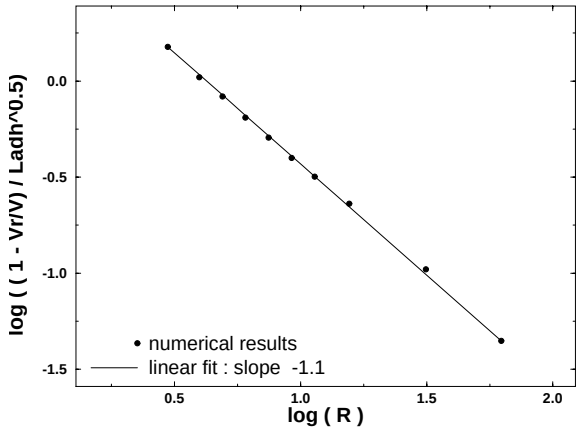

Fig. 18. Variation of the vesicle size at constant reduced volume. (Numerical values: $R = 0.5 \to 10$, $Rs/R = 0.96$, $R_{\rm c} = 0.4$, $d_0 = 0.06$.)

The local velocity in the thin fluid film under the vesicle is $V - V_{\rm r}$ and the velocity vanishes on a distance d_0. This leads to the following local dissipation (see Fig. 17)

$$D_{\rm loc} \sim \eta\, L_{\rm adh}\, d_0 \left(\frac{V-V_{\rm r}}{d_0}\right)^2. \qquad (56)$$

Equating this dissipation with that given in (49) we obtain:

$$1 - \frac{V_{\rm r}}{V} \sim \frac{\sqrt{L_{\rm adh} d_0}}{R}. \qquad (57)$$

A remark is in order, however. If we use the law $L_{\rm adh} \sim R_{\rm c}^{-2/5}$ valid in 2D and small adhesion regime (19), one would get that $1 - V_{\rm r}/V \sim R_{\rm c}^{-1/5}$. This means that rotation would increase with rigidity ($R_{\rm c} \sim \sqrt{\kappa/w_0}$). Since an increase of κ reduces $L_{\rm adh}$, we see from equation (57) that rotation would be higher on decreasing $L_{\rm adh}$, which is in contradiction with expectation. In order to remedy this apparent contradiction one must keep in mind that, as for the translational velocity (51), our scaling relation holds if the other parameters are fixed. In other words, the scaling law contains a dimensionless prefactor of the form $f(d_0/R_{\rm c}, R_{\rm s}/R)$, the determination of which is performed numerically as presented below.

6.3.2 Numerical results

We have made an extensive numerical analysis (see Figs. 18, 19 and 20), and arrived to the conclusion that the

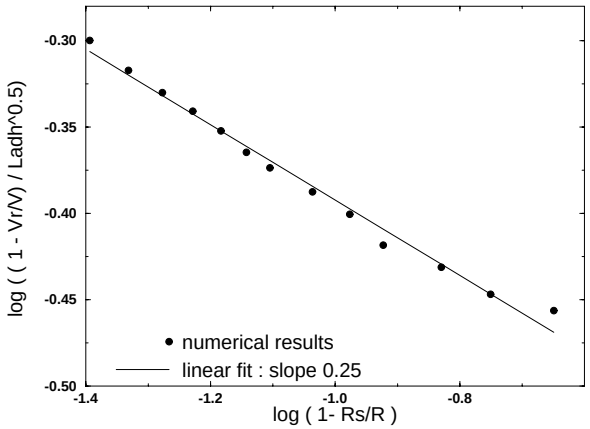

Fig. 19. Variation of the reduced volume. (Numerical values: $Rs/R = 0.78 \rightarrow 0.95$, $R = 1.1$, $R_c = 0.5$, $d_0 = 0.06$.)

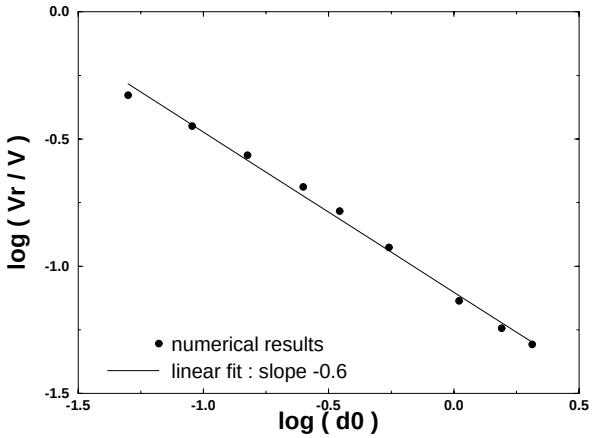

Fig. 20. Variation of potential range. (Numerical values: $Rs/R = 0.88$, $R = 1.1$, $R_c = 0.6$, $d_0 = 0.05 \rightarrow 2$.)

quantity measuring the rotation rate takes the form

$$\tau_s \sim \frac{F}{\eta}\frac{\sqrt{L_{adh} d_0}}{R}\left(1 - \frac{R_s}{R}\right)^{-0.25} h\left(\frac{d_0}{R_c}\right). \qquad (58)$$

The first factor is the one given in equation (57). The dependence in d_0 does not appear clearly in this equation. The remaining unknown function h seems not to have a simple analytical expression. Nevertheless we were able to determine the scaling behavior of the rotation rate $1 - \tau_s$ for the parameter d_0 (Eq. (59)). The result is the same as for a cylinder

$$1 - \tau_s \sim \frac{1}{\sqrt{d_0}}. \qquad (59)$$

A quite large region of parameter space has been explored numerically, leading to a very good agreement with the analytical predictions.

7 Summary and conclusion

In this section we summarize the main findings of this paper and discuss some future issues.

- We have solved the full 2D problem including hydrodynamics. This has allowed us to study various situations, though here most of our reasoning has been exemplified for haptotaxis.
- We have shown that during motion the vesicle moves with a translational velocity and has a rotation component.
- We have developed a general analytical study based on dimensional and scaling analyses. Firstly, we have analyzed the adhesion area behavior, a quantity which plays a central role in dynamics. We have distinguished between the tense and flask regime.
- Analyzing the dissipation and the power we have derived scaling laws for the migration velocity. In the tense regime we recover the Stokes law, while in the flask regime we discover a new scaling law. In 3D the Stokes law is modified: instead of $V \sim 1/R$ we have $V \sim 1/R^2$, V is the velocity and R the size.
- Based on the same kind of arguments we have derived the rotation/translation ratio.
- In a generally coherent picture we have analyzed the effect of the swelling as well as the distance from the substrate. Our numerical results are in good agreement with the analytical results.

Several issues have not been addressed in this paper and they should constitute a task for future investigations. (i) Firstly, we have disregarded dissipation due to bond breaking and restoring with the substrate. In situations where specific adhesion is present, this question becomes essential. In particular one expects that the velocity becomes a nonlinear function with the driving force due to the discreteness of the adhesion potential. (ii) A second important point is the extension of the present analysis to 3D with regard to numerical calculations. (iii) In order to mimic the dynamics of more sophisticated entities in biology, one must go further beyond in the complexity. For example, in order to take into account the cytoskeletton we need to take into consideration the appropriate rheological law for the membrane (for example the rheological law of the type of Mooney [40] used to model the red blood cell). (iv) In general not only the membrane rheology matters, but also the interior of the cell. For example the cell responds according to a viscoelastic law of non Newtonian type. These questions must be progressively incorporated if one wishes to have a more realistic description of complex objects. Of course the integral formulation can not be used in general due to the nonlinearity of the constitutive equations, and one has to resort to a new method, namely the advected-field (or phase-field) approach as recently introduced [11].

C.M. is grateful to the Centre National des Études Spatiales (CNES) for a financial support. The work of K.K. and C.M. is supported by the French-German cooperation program PROCOPE.

References

1. W. Helfrich, Z. Naturforsch. C **28**, 693 (1973)
2. *Structure and Dynamics of Membranes, Handbook of Biological Physics*, edited by R. Lipowsky, E. Sackmann (Elsevier, North-Holland, 1995)
3. J. Prost, R. Bruinsma, Europhys. Lett. **33**, 321 (1996)
4. M. Kraus, W. Wintz, U. Seifert, R. Lipowsky, Phys. Rev. Lett. **77**, 3685 (1996)
5. I. Durand *et al.*, Phys. Rev. E **56**, 3776 (1997)
6. I. Cantat, C. Misbah, Phys. Rev. Lett. **83**, 235 (1999)
7. N. Kern, B. Fourcade, Europhys. Lett. **46**, 262 (1999)
8. I. Cantat, C. Misbah, Phys. Rev. Lett. **83**, 880 (1999)
9. U. Seifert, Phys. Rev. Lett. **83**, 876 (1999)
10. S. Sukumaran, U. Seifert, Phys. Rev. E **64**, 011916 (2001)
11. T. Biben, C. Misbah, Euro. Phys. J. B **29**, 311 (2002)
12. J. Nardi, R. Bruinsma, E. Sackmann, Phys. Rev. Lett. **82**, 5168 (1999)
13. M. Abkarian, C. Lartigue, A. Viallat, Phys. Rev. E **63**, 041906 (2001)
14. B. Lortz, R. Simon, J. Nardi, E. Sackmann, Europhys. Lett. **51**, 468 (2000)
15. M. Abkarian, C. Lartigue, A. Viallat, Phys. Rev. Lett. **88**, 068103 (2002)
16. I. Cantat, C. Misbah, *Transport versus Structure in Biological and Chemical Systems*, S. Verlag, edited by S. Müller *et al.* (1999)
17. I. Cantat, C. Misbah, Y. Saito, Euro. Phys. J. E **3**, 403 (2000)
18. J.O. Rädler, T.J. Feder, H.H. Strey, E. Sackmann, Phys. Rev. E **51**, 4526 (1995)
19. E. Evans, D. Berk, A. Leung, Biophys. J. **59**, 838 (1991)
20. D. Braun, P. Fromherz, Phys. Rev. Lett. **81**, 5241 (1998)
21. A. Kloboucek, A. Behrisch, J. Faix, E. Sackmann, Biophys. J. **77**, 2311 (1999)
22. Z. Csahók, C. Misbah, A. Valance, Physica D **128**, 87 (1999)
23. A.L. Bernard, Ph.D. Thesis, Thèse de doctorat de l'Université Paris 6, Paris, 1999
24. J. Farinas, A.S. Verkman, Biophys. J. **71**, 3511 (1996)
25. U. Seifert, R. Lipowsky, Phys. Rev. A **42**, 4768 (1990)
26. U. Seifert, Phys. Rev. A **43**, 6803 (1991)
27. R. Bruinsma, in *Physics of Biomaterials, Fluctuations, Self Assembly and Evolution*, edited by T. Riste, D. Sherrington (Kluwer, NATO ASI Series 332, Dodrecht, 1996), p. 61
28. L. Mahadevan, Y. Pomeau, Physics of Fluids **11**, 2449 (1999)
29. F. Brochard, J.-F. Lennon, J. Phys. France **36**, 1035 (1975)
30. The velocity field behavior at long distance can not be obtained with our method, but has no influence on the vesicle motion as shecked theoretically in paragraph 4.4 and numerically. Especially, the expected velocity decay at long distance is not observed numerically. This is due to the fact that the total force exerted on the fluid, which is theoretically zero in the Stokes limit, is numerically only very close to zero. This small numerical error on the forces becomes dominant at long distance and induces artificial logarithmically diverging velocities
31. A. Yeung, E. Evans, J. Phys. II France **5**, 1501 (1995)
32. U. Seifert, S.A. Langer, Europhys. Lett. **23**, 71 (1993)
33. A. Albersdörfer, R. Bruinsma, E. Sackmann, Europhys. Lett. **42**, 227 (1998)
34. C.W. Oseen, *Hydrodynamics* (Akademische Verlag, Leipzig, 1927)
35. J.R. Blake, Proc. Camb. Phil. Soc. **70**, 303 (1971)
36. L.D. Landau, E. Lifchitz, *Fluid Mechanics* (Pergamon, Oxford, 1959)
37. D.J. Jeffrey, Y. Onishi, Q.J. Mech, Appl. Math. **34**, 129 (1981)
38. W.H. Press, B.P. Flannery, S.A. Teukolsky, W.T. Vetterling, *Numerical Recipes* (Cambridge University Press, Cambridge, 1986)
39. A.J. Goldman, R.G. Cox, H. Brenner, Chem. Eng. Science **22**, 637 (1967)
40. M. Mooney, J. Appl. Phys. **11**, 582 (1940)